Journal Name

COMMUNICATION

Designed Intramolecular Blocking of the SCO of an Fe(II) Complex

C. Bartual-Murgui,[a,*] S. Vela,[b,*] O. Roubeau[c] and G. Aromí[a,*]

Received 00th January 20xx,
Accepted 00th January 20xx

DOI: 10.1039/x0xx00000x

www.rsc.org/

A ligand derived from 1,3bpp (2-(pyrazol-1-yl)-6-(pyrazol-3-yl)-pyridine) has been prepared to proof that the SCO of an Fe(II) complex can be blocked by means of intramolecular interactions not related to the crystal field. Calculations show that the blocking is caused by the energy penalty incurred by the rotation of a phenyl ring, needed to avoid steric hindrance upon SCO.

The exploitation of spin crossover (SCO) offers an opportunity for implementing a molecular-based switching property at the nano-scale.[1-3] The phenomenon is displayed by transition metals that exhibit two possible *d* electron configurations, and a ligand field causing these to lye close in energy, so that they can be easily interconverted through external stimuli. The spin transition occurs along changes to the structure, together with variations to physical properties such as colour,[4] magnetic[5-7] or electrical[8] properties, mechanical responses,[9] etc. The dynamics of the spin transition, crucial for exploiting the switching behaviour, are governed by elastic interactions between active centres within the crystal host lattice. Thus, the presence of a dense network of intermolecular or covalent interactions often leads to cooperative SCO, which translates into abrupt transitions, sometimes accompanied by hysteresis.[10, 11] Therefore, great efforts are dedicated to unveil the subtle links between SCO and the associated changes to the crystal lattice.[12-14] In this context, structural analyses indicate that complexes with the appropriate ligand field to undergo SCO may be kinetically trapped in the high spin (HS) state if the transition requires excessive crystal lattice rearrangement energy, which is usually gauged by a very distorted coordination geometry.[15, 16] This was also demonstrated by means of DFT + *U* calculations in the solid state.[17] Complementary to this, from studying the Fe(II) complexes of a family of indazolylpyridine ligands, it was proposed that the relative stability of the HS and low spin (LS) states may be strongly modulated by intra-ligand steric interactions.[18] In a theoretical investigation, it was suggested that the true reason for the drastic differences within that series of compounds are indeed inter-ligand (while intra-molecular) steric factors.[19] With the aim of exploiting these factors, we have designed a ligand that serves to demonstrate that a complex expected to show SCO can be completely blocked into the HS state by virtue of purely intra-molecular, non-covalent interactions and not due to a lattice effect. A thorough DFT analysis provides an elegant rationalization of this behaviour.

The new ligand Ph1,3bpp (2-(3-phenylpyrazol-1-yl)-6-(1H-pyrazol-3-yl)-pyridine; Scheme I) was prepared in three steps, starting with the coupling of 3-phenylpyrazol with 2-acetyl-6-bromopyridine, followed by isolation of the corresponding propanone intermediate that results from activation of the acetyl group with 1,1-dimethoxytrimethylamine, which upon ring-closure with hydrazine yields the desired product (SI).

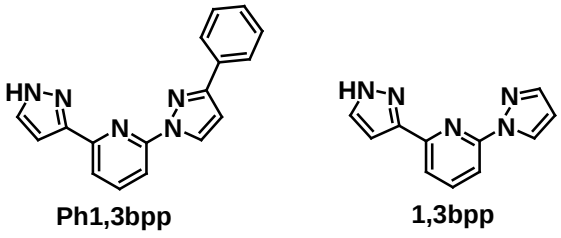

Scheme I. Molecular structure of ligands Ph1,3bpp and 1,3bpp.

The reaction of Ph1,3bpp with $Fe(ClO_4)_2{\cdot}6H_2O$ in dry acetone produced crystals of the compound $[Fe(Ph1,3bpp)_2](ClO_4)_2{\cdot}C_3H_6O$ (**1a**) upon layering the initial mixture with Et_2O. Compound **1a** crystallizes in the orthorhombic space group $Pca2_1$. The asymmetric unit (Fig. S1) contains two entire formula units, which are very similar but not crystallographically equivalent. The unit cell includes four asymmetric units. Crystallographic data and metric parameters can be found at

[a] *Departament de Química Inorgànica i Orgànica and IN2UB, Universitat de Barcelona, Diagonal 645, 08028 Barcelona, Spain.*
[b] *Laboratoire de Chimie Quantique, Université de Strasbourg, 4 rue Blaise Pascal, F-67000 Strasbourg, France.*
[c] *Instituto de Ciencia de Materiales de Aragón (ICMA), CSIC and Universidad de Zaragoza, Plaza San Francisco s/n, 50009 Zaragoza, Spain.*

Electronic Supplementary Information (ESI) available: Ligand synthesis details, crystallographic tables and additional figures, PXRD patterns, TGA graphs, additional magnetocaloric graphs. See DOI: 10.1039/x0xx00000x

the SI. The basic unit of **1a** comprises a $[Fe(Ph1,3bpp)_2]^{2+}$ complex cation with the charge compensated by two ClO_4^- anions and one molecule of acetone of crystallization (Fig. 1). The complex consists of an Fe(II) centre coordinated by two tridentate Ph1,3bpp ligands in *mer* fashion, completing a very distorted FeN_6 coordination geometry. The average of the Fe–N bond distances are 2.16(4) Å, for the two different Fe(II) ions, respectively, which shows that both of them remain in the HS state at 100 K, here as a result of intra-molecular, inter-ligand interactions (see below). The severe distortion of the metal environment from the ideal octahedron as gauged by the parameters ∑ and Θ[7] (here with average ∑ and Θ values of 168.8(9) and 521(2), respectively) also witnesses the HS state.[20]

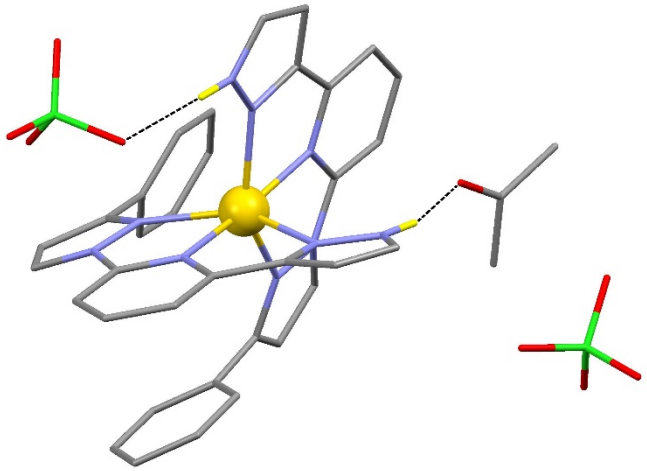

Figure 1. Molecular representation of one of the formula units in $[Fe(Ph1,3bpp)_2](ClO_4)_2{\cdot}C_3H_6O$ (**1a**). Fe is the yellow ball, C is grey, N is purple, O is red, Cl is green. Only H atoms of N–H groups shown (in yellow). Dashed lines are H-bonds.

The conformation of the Ph1,3bpp ligands within the complex must be emphasized; the phenyl substituent is in all cases twisted with respect to its adjacent pyrazolyl ring with angles 47.71/46.56° and 49.24/47.75°, (Fig S2), and is establishing an intramolecular π···π interaction with the 1,3bpp fragment of the other ligand in the complex. These two factors likely play a role in the pronounced mutual rotation of both 1,3bpp moieties away from orthogonality (angles between idealized planes of 69.79 and 71.53°). The N–H groups of the complex interact through strong hydrogen bonds with the acetone molecule and one perchlorate anion, respectively. The other ClO_4^- group in the formula is subject to weaker interactions within the lattice. This happens for both complexes of the asymmetric unit. The complexes are disposed in sheets that contain both possible enantiomers, where they interact with each other only *via* C–H···π interactions (Fig. S3). Thus, the organization within these sheets does not follow the compact network of C–H···π and π···π contacts known as the "terpy embrace" usually encountered in complexes with bpp type ligands.[21] Acetone and ClO_4^- anions are located in between the sheets of complexes, yielding a lattice that alternates essentially hydrophobic with rather hydrophilic layers (Fig. S4). The sheets of metal complexes feature two significantly different separations (amounting to 9.368 and 12.190 Å, respectively). Half of the ClO_4^- anions in the compound and all the molecules of acetone are located at the space between metallic complex layers with largest separation, whereas the remaining anions lie in the other inter-sheet domain (Fig. 2). Upon exposure to the atmosphere, compound **1a** exchanges all its acetone content with half equivalent of water molecules, in a single-crystal-to-single-crystal (SCSC) manner. This transformation does not lead to any apparent changes while single-crystal X-ray diffraction allows the determination of the molecular structure of the new product; $[Fe(Ph1,3bpp)_2]$ $(ClO_4)_2{\cdot}0.5H_2O$ (**1b**). Thermogravimetric analyses (TGA) also confirm the process (Fig. S5). This system joins a growing family of bpp-based Fe(II) complexes that experience SCSC solvent exchange processes allowing the use of SCXRD to study the initial and the final forms,[22-25] and sometimes even intermediate phases.[26] Compound **1b** is found in the orthorhombic space group $Pna2_1$, its asymmetric unit (Fig. S6) comprising two inequivalent $[Fe(Ph1,3bpp)_2]^{2+}$ complexes, four ClO_4^- ions and one molecule of water. The latter occupies a position equivalent to one of the acetone molecules in **1a**, also forming a H-bond with one N–H group. The remaining N–H groups that were interacting with the other acetone in **1a** are now donors of a H-bond with one ClO_4^- ion. Therefore, after the molecular movements occurring during the **1a** → **1b** transformation, one third of the ClO_4^- groups are now involved in N–H···$O(ClO_3)^-$ interactions. This molecular exchange does not lead to significant changes to the conformation and structural parameters of the $[Fe(Ph1,3bpp)_2]^{2+}$ moieties (see SI), which also remain, as expected, in the HS state at 100 K (average Fe–N distances of 2.166(11) and 2.165(11) Å). Likewise, the layered organization of the complex cations within the crystal lattice does not vary. The sheets are separated by the perchlorate groups, featuring two types of separations (now of 9.422 and 10.551 Å, respectively). The larger interlayer domain also includes the molecules of water (Fig. 2). It is thus clear that the space located in between the largest inter-layer separation mediates the diffusion of molecules transiting in and out the lattice. The exchange process causes a 9% contraction of the lattice.

Contrary to most SCSC small-molecule exchanges reported for the family of bpp/Fe(II) complexes,[22-25] the **1a** → **1b** transformation does not produce a spin switching (at least down to 100 K) from the HS state. This was corroborated by means of magnetic susceptibility measurements down to 5 K (Fig. S7). Thus, under a constant magnetic field of 0.1 T, compounds **1a** and **1b** exhibit a value of the $\chi_M T$ product (χ_M is molar paramagnetic susceptibility) of 4.04 and 3.94 cm^3Kmol^{-1} at 350 and 301 K, respectively, consistent with both systems being completely in the HS state (S=2). The Curie Law behaviour holds in both cases down to below 50 K, from where the curves $\chi_M T$ *vs.* T plots exhibit the sharp expected decline resulting from zero field splitting effects on HS Fe(II).

Ligand Ph1,3bpp was designed to proof that intramolecular interactions could be exploited to block the SCO and trap a complex in the HS state. The magnetic response of **1a** and the fact that the exchange acetone/water does not affect this response point in this direction. For comparison, the related complex $[Fe(1,3bpp)_2](ClO_4)_2$ (**2**),[27] which features the same core as **1a** and **1b** without the Ph substituent, exhibits a complete SCO near 275 K (Fig. S7), which also supports this hypothesis. An elegant explanation for the SCO blocking of **1a** and **1b** was given by means of computational tools. Thus, the optimized geometries associated to the HS and hypothetical LS states of complex $[Fe(Ph1,3bpp)_2]^{2+}$ (**1**) in gas-phase conditions were determined, starting from crystal coordinates (Fig. S8). The calculated HS structure ($\mathbf{1}_{HS}$) is very similar to the experimental one, reproducing the Fe–N distances, and most notably, the distortion of the coordination geometry (average

Fe–N distance, 2.191 Å; ∑ = 165.04; Θ = 530). The structure obtained for the hypothetical LS state ($\mathbf{1}_{LS}$) features the expected compression of the FeN_6 core (average Fe–N value, 1.963 Å), which also becomes closer to an ideal octahedron ∑ = 99.26; Θ = 308). Interestingly, in both cases, the phenyl substituents of the ligands are twisted with respect to their respective 1,3bpp planes (Fig. S8), as also observed experimentally. This could be ascribed to a tendency for establishing favourable inter-ligand π···π interactions (see below). The calculated energies of both forms predict higher electronic enthalpy for $\mathbf{1}_{HS}$ (ΔH_{elec} = –1.7 kJmol^{-1}), which would indeed preclude the thermal SCO, since the latter is an entropy driven process. In order to compare with **2**, single point energy evaluations were performed on $\mathbf{1}_{HS}$ and $\mathbf{1}_{LS}$ without the phenyl substituents. This results in a dramatic inversion of the relative HS *vs* LS electronic enthalpies, now giving ΔH_{elec} = +10.8 kJmol^{-1} and restoring the thermodynamic stability of the LS state, consistent with the experimental results.[27] Both sets of calculations confirm that the blocking of the SCO in **1** is entirely related to the phenyl groups. The influence of the intramolecular π···π interaction was examined using several models. It was found that this interaction causes a difference in stability of only –0.1 to –0.5 kJmol^{-1} in favor of the HS state. Such contribution is nearly two orders of magnitude smaller than the overall effect of *ca.* 12 kJmol^{-1} caused by the Ph rings (by adding ΔH_{elec} in systems **1** and **2**, *ie* –1.7 and 10.8 kJmol^{-1}). Another difference between $\mathbf{1}_{HS}$ and $\mathbf{1}_{LS}$, also related with the phenyl substituent of Ph1,3bpp, is the torsion angle between this substituent and their carrier pyrazolyl rings, with average values of 35.58° ($\mathbf{1}_{HS}$) and 51.26° ($\mathbf{1}_{LS}$). The theoretical analysis of the energy of a phenylpyrazol moiety as function of the torsion angle unveils a significant destabilization of the system as it is removed from planarity by rotation about the C–C bond between both rings (Fig. 3), which indicates that this factor would favour the HS state. From this calculation, a change from 35° to 50°, as observed in the optimized structures, corresponds to a loss of *ca.* 4 kJmol^{-1}.

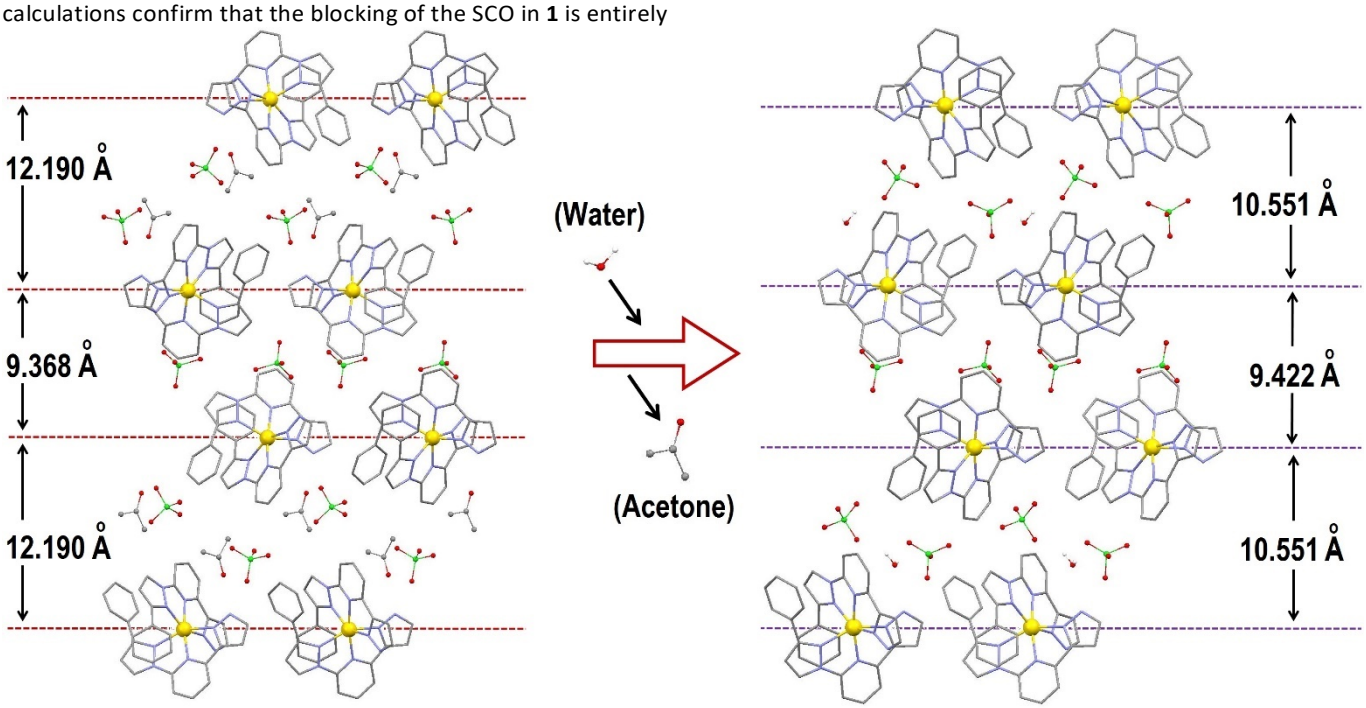

Figure 2. View of the lattices of **1a** (left) and **1b** (right) down the crystallographic *b* axis, emphasizing the solvent exchange that takes one into the other and the two interlayer separations hosting or not the migrating molecules. Code: balls, Fe; red, O; green, Cl; grey, C. Hydrogen not shown.

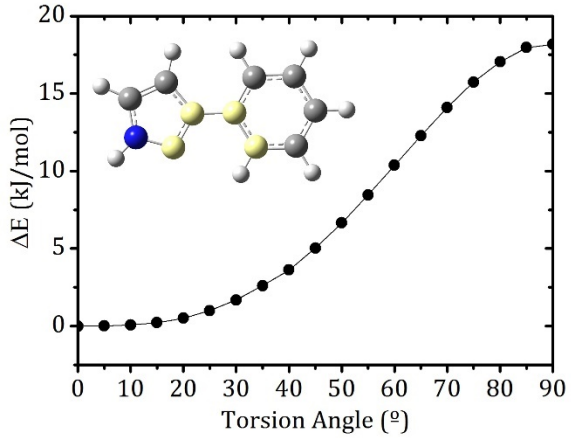

Figure 3. Computed energy variation of a phenylpyrazole moiety as a function of the torsion angle between both aromatic rings, as gauged by the torsion angle featured by the four atoms highlighted in yellow in the inset.

Considering that **1** contains two such units, the effective stabilization of $\mathbf{1}_{HS}$ on this account would be *ca.* 8 kJmol^{-1}, close to the calculated *ca.* 12 kJmol^{-1} HS *vs.* LS energy difference related to the Ph ring. The reason for an increased planarity loss upon HS to LS transition is the added steric hindrance between ligands generated with the compression of the FeN_6 core (Fig. S8). The absence of this additional rotation would force, in the LS state, the presence of a 2.3 Å C···H contact, in addition to other C···C, C···H or H···H contacts near 2.5 Å, extremely unfavorable energetically. This analysis clearly indicates that the reason why the HS state is blocked for compounds **1a** and **1b** is the energy penalty that would signify the additional rotation of the Ph group upon SCO, as the only mechanism to avoid intramolecular, inter-ligand steric hindrance. The fact that the torsion angles observed in **1a** and **1b** are larger than predicted in the calculations for $\mathbf{1}_{HS}$ could be ascribed to the electronic differences of the real system with respect to the phenylpyrazol model, rendering the former more tolerant to

the torsion. However, the need to overcome a "torque" energy upon SCO remains the same.

In summary, ligand Ph1,3bpp, featuring a Ph substituent to the 1,3bpp core, was prepared in order to show that the SCO of an Fe(II) chromophore could be blocked by only intramolecular forces, with no effect from the crystal field. The new compound $[Fe(Ph1,3bpp)_2]$ $(ClO_4)_2 \cdot C_3H_6O$ (**1a**) undergoes a SCSC complete exchange of lattice acetone molecules by H_2O in the atmosphere, yielding $[Fe(Ph1,3bpp)_2]$ $(ClO_4)_2 \cdot 0.5H_2O$ (**1b**). Both solvatomorphs retain the HS state down to 5 K, unlike compound $[Fe(1,3bpp)_2](ClO_4)_2$ (**2**), made with the parent ligand. Theoretical calculations of $[Fe(Ph1,3bpp)_2]^{2+}$ in the gas phase show that indeed its optimized structure in the LS state is less stable than in the HS one because the Ph group needs to rotate to alleviate the steric hindrance caused by the neighboring ligand. The rotation implies an energetic penalty associated to the loss of planarity in the phenyl-pyrazole-3-yl group. This provides for an elegant rationalization of the intramolecular based SCO inhibition, which here is thermodynamic and not kinetic, as rationalized theoretically[17] for systems were the blocking is based on intermolecular interactions.

The authors thank the Generalitat de Catalunya for the prize ICREA Academia 2008 and 2013, the ERC for Starting Grant StG-2010-258060 (GA), MINECO for grants MAT2014-53961-R (OR), MAT2015-70868-ERC (OR), CTQ2012-32247 (GA) and CTQ2015-68370-P (GA, CBM), LabEx-Chemistry of Complex Systems for post-doctoral grant ANR-10-LABX-0026CSC (SV) and the regional High-Performance Computing (HPC) center in Strasbourg for computational resources (SV).

Notes and references

1. *Spin-Crossover Materials*, John Wiley & Sons Ltd, 2013.
2. P. Gamez, J. Sanchez Costa, M. Quesada and G. Aromí, *Dalton Trans.*, 2009, 7845-7853.
3. A. Bousseksou, G. Molnar, L. Salmon and W. Nicolazzi, *Chem. Soc. Rev.*, 2011, **40**, 3313-3335.
4. O. Kahn, J. Krober and C. Jay, *Adv. Mater.*, 1992, **4**, 718-728.
5. K. S. Murray, *Eur. J. Inorg. Chem.*, 2008, 3101-3121.
6. J. A. Real, A. B. Gaspar and M. C. Munoz, *Dalton Trans.*, 2005, 2062-2079.
7. P. Gutlich and H. A. Goodwin, *Top. Curr. Chem.*, 2004, **233**, 1-47.
8. C. Lefter, V. Davesne, L. Salmon, G. Molnár, P. Demont, A. Rotaru and A. Bousseksou, *Magnetochemistry*, 2016, **2**, 18.
9. M. D. Manrique-Juarez, S. Rat, L. Salmon, G. Molnar, C. M. Quintero, L. Nicu, H. J. Shepherd and A. Bousseksou, *Coord. Chem. Rev.*, 2016, **308**, 395-408.
10. M. A. Halcrow, *Chem. Lett.*, 2014, **43**, 1178-1188.
11. J. A. Real, A. B. Gaspar, V. Niel and M. C. Munoz, *Coord. Chem. Rev.*, 2003, **236**, 121-141.
12. M. Shatruk, H. Phan, B. A. Chrisostomo and A. Suleimenova, *Coord. Chem. Rev.*, 2015, **289**, 62-73.
13. N. Ortega-Villar, M. Muñoz and J. Real, *Magnetochemistry*, 2016, **2**, 16.
14. G. A. Craig, J. Sanchez Costa, O. Roubeau, S. J. Teat and G. Aromí, *Chem., Eur. J.*, 2011, **17**, 3120-3127.
15. M. A. Halcrow, *Chem. Soc. Rev.*, 2011, **40**, 4119-4142.
16. G. A. Craig, J. Sanchez Costa, O. Roubeau, S. J. Teat and G. Aromí, *Chem., Eur. J.*, 2012, **18**, 11703-11715.
17. S. Vela, J. J. Novoa and J. Ribas-Arino, *Phys. Chem. Chem. Phys.*, 2014, **16**, 27012-27024.
18. A. Santoro, L. J. K. Cook, R. Kulmaczewski, S. A. Barrett, O. Cespedes and M. A. Halcrow, *Inorg. Chem.*, 2015, **54**, 682-693.
19. S. Vela, C. Gourlaouen, M. Fumanal and J. Ribas-Arino, *Magnetochemistry*, 2016, **2**, 6.
20. M. A. Halcrow, *Coord. Chem. Rev.*, 2009, **253**, 2493-2514.
21. G. A. Craig, O. Roubeau and G. Aromí, *Coord. Chem. Rev.*, 2014, **269**, 13-31.
22. L. A. Barrios, C. Bartual-Murgui, E. Peyrecave-Lleixà, B. Le Guennic, S. J. Teat, O. Roubeau and G. Aromí, *Inorg. Chem.*, 2016, **55**, 4110-4116.
23. D. Gentili, N. Demitri, B. Schafer, F. Liscio, I. Bergenti, G. Ruani, M. Ruben and M. Cavallini, *J. Mater. Chem. C*, 2015, **3**, 7836-7844.
24. L. J. K. Cook, R. Kulmaczewski, O. Cespedes and M. A. Halcrow, *Chem., Eur. J.*, 2016, **22**, 1789-1799.
25. J. Sánchez Costa, S. Rodríguez-Jimenez, G. A. Craig, B. Barth, C. M. Beavers, S. J. Teat and G. Aromí, *J. Am. Chem. Soc.*, 2014, **136**, 3869-3874.
26. G. Aromí, C. M. Beavers, J. Sanchez Costa, G. A. Craig, G. Minguez Espallargas, A. Orera and O. Roubeau, *Chem. Sci.*, 2016, **7**, 2907-2915.
27. C. Bartual-Murgui, C. Codina, O. Roubeau and G. Aromí, *Chem., Eur. J.*, 2016, *in press.*

